

A NETWORK OF DISDROMETERS TO QUANTIFY THE SMALL-SCALE VARIABILITY OF THE RAINDROP SIZE DISTRIBUTION

Joël Jaffrain*, Alexis Berne, André Studzinski and Florian Pantillon

Laboratoire de Télédétection Environnementale,
École Polytechnique Fédérale de Lausanne, Switzerland

1 INTRODUCTION

The *(rain)drop size distribution* (DSD hereafter) is a statistical way to summarize the information on the microstructure of rain which is of primary importance to estimate bulk variables describing rainfall. Similarly to rain, DSD is highly variable in time and space. The accuracy of rain estimates from weather radar is affected by the variability of DSD at all scales. Previous studies have investigated the effect of temporal variability of the DSD on radar rain estimation selecting different types of rain events (stratiform, transitional phase, convective) (e.g., Tokay and Short, 1996; Uijlenhoet et al., 2003; Lee and Zawadzki, 2005). This variability can result in important biases in rain rate estimates (in the order of 40%) especially if the physical processes involved are not well identified (Lee and Zawadzki, 2005). DSD spectra are collected at the ground level using disdrometers (electro mechanical, optical or video type). Such measurements provide point information but are not representative of the surrounding area, in particular for rain highly variable in space. Spatial variability of the DSD can be investigated using multiple measurements distributed in the same area. Miriovsky et al. (2004) highlighted the difficulty to distinguish between natural variability of DSD and instrumental effects when using instruments of different types. More recently, the variability of the DSD over 1.3 km of distance was shown to yield an average error of 25% in the estimation of rain accumulation (Lee et al., 2009). Nevertheless, because of the limited spatial distribution of the instruments, the collected data were not sufficient to fully understand the spatial variability.

The objectif of this work is to design and set up a network of disdrometers over a $1 \times 1 \text{ km}^2$ area, corresponding to the typical pixel of an operational radar. The network and its components are presented in details in Section 2 while preliminary analyses of the DSD variability are provided in Section 3.

* *Corresponding author address:* Joël Jaffrain, LTE, Station 2, EPFL, 1015 Lausanne, Switzerland;
e-mail: joel.jaffrain@epfl.ch

2 EXPERIMENTAL SET UP

2.1 Network Architecture

The network was designed to be easily deployed without the usual restrictions on power supply or data management. It consists of 16 sensing stations designed for autonomous functioning in terms of power supply and data transfer, providing DSD measurements as well as integrated parameters (rain rate, radar reflectivity factor), information about precipitation type and additional technical information about the sensor at a high temporal resolution of 30 s. The number of stations was defined as the best trade-off between a sufficient density of points for reliable spatial investigations and the cost of the project. The network was fully deployed over EPFL campus in Lausanne, Switzerland, in mid-March 2009. This region has temperate wet continental climate. The 16 stations are more or less regularly distributed on the roof of EPFL buildings in order to cover an area of about $1 \times 1 \text{ km}^2$ (Figure 1). To prevent possible wind disturbances induced by the buildings (“edge effects”), the stations were deployed as far as possible from the edges of the roofs. In addition, local winds have limited speed (usually below 5 m s^{-1}) and hence edge effects are supposed to be negligible. The following sections describe in details the components of this network from the measuring sensor to the overall network.

2.2 From Optical Disdrometer to autonomous station

Parsivel® (manufactured by OTT) is an optical disdrometer (Löffler-Mang and Joss, 2000) with a sampling area of 54 cm^2 providing DSD measurements as well as parameters derived from the DSD, i.e., rain rate R and radar reflectivity factor Z , and information on precipitation type. The instrument consists of a transmitter and a receiver separated by a 54 cm^2 laser beam (see Figure 2). The measuring principle is based on the attenuation of the signal when a particle crosses the sampling laser beam. The instrument provides the number of drops according to their respective equivolumetric diameter and terminal fall velocity. The ranges of sizes (from



Figure 2: The optical disdrometer Parsivel (OTT) providing DSD measurements based on the attenuation of the laser signal when a particle crosses the beam.

0.25 to 25 mm) and velocities (from 0 to 20 m s⁻¹) are divided into 32 non-equidistant classes each.

In order to be easily deployed, the sensors have to be autonomous in terms of power supply as well as data storage/transmission. The system is running

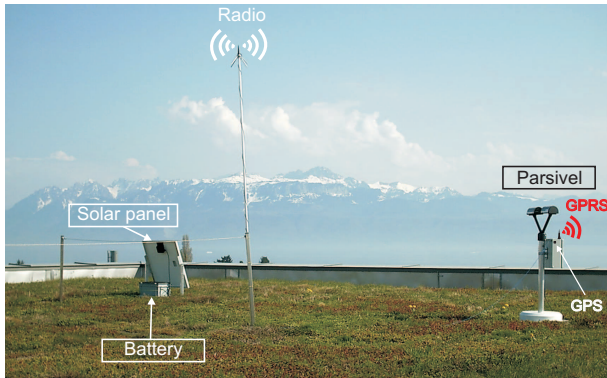


Figure 3: A wireless autonomous station for DSD measurement. The station consists of a measuring sensor, the electronic unit managing power and data transmission, the battery and the solar panel.

on a 12 V battery which is connected to a 65 W solar panel. In the following, the term *station* denotes the ensemble made of the instrument, the electronic and transmission units, the solar panel and the battery (Figure 3).

2.3 Data Collection and Storage

For data storage, the Campbell Scientific® data logger CR1000 was selected because of its capabilities to manage four different inputs. The CR1000

is equipped with a CompactFlash memory module CFM100 and a 2 GB card. For cost reasons, all 16 stations of the network cannot be equipped with a data logger. Consequently, the network is organized around four data loggers, each one managing data from four stations. The network is hence divided in four groups of 4 stations. Each group is lead by the station equipped with the data logger, denoted as *master station*. To avoid transmission failure, each group is using its own range of frequencies. Within a time step of 30 s, the master station queries successively data to the three slaves of the same group through radio communication. In case of transmission failure, the master can repeat up to 8 times the operation. This collection phase can last up to 10 s. The remaining 20 s are devoted to the transmission of the 4 measurements to a remote web server centralizing data using GPRS connection. The memory card is not required when using GPRS but is used as backup if problems happen on GPRS. Given the size of a complete measurement, about 5 KB for each sensor, the autonomy of the 2 GB memory card in case of transmission failure is about 30 days. The clock of each data logger is synchronized every day at midnight using the GPS receiver included in the GPRS module.

Hence, the remote server receives data from the 4 master stations every 30 s. The last transmitted data are shown on the web server page in order to check that all data were successfully transmitted. Once a day, data are remotely downloaded and stored. Near real-time access to data is very useful to quickly detect technical failures within the network.

3 PRELIMINARY RESULTS

3.1 Method and Data Set

The network has been running for several months and data corresponding to different types of rain events have been collected. In order to keep this paper short, only one rain event that occurred on the 3rd of September 2009 is selected for illustration. It lasted 1.5 h from 23:15 to 00:45 (GMT). The rain signal measured by each station of the network is presented in Figure 4. The maximum rain rate is about 200 mm h⁻¹ at 23:50. The average rain amount over the 16 stations is about 14.5 mm. The deviation of the 16 individual amount values from the mean is in the range $\pm 10\%$. A maximum drop diameter of about 5.5 mm was recorded during the peak of the event. The maximum drop concentration during the peak was about 3000 m⁻³mm⁻¹ for drop diameters of about 0.4 and 0.5 mm. The DSD

spectra of each station are presented as a function of time in Figure 5.

Data have been filtered in order to have all the 16 stations providing a measurement (i.e. no missing measurement due to data transmission failure is allowed) at the considered time step. Moreover, non-rainy period, i.e., when less than three stations record a positive rain rate at the same time, were removed before the analysis.

3.2 Variability of the parameters of the Gamma distribution

Figure 5 shows the observed variability of DSD during the event as well as within the typical radar pixel area. One way to quantify this variability is to fit a Gamma distribution on each DSD spectrum recorded at each time step. The Gamma distribution (Ulbrich, 1983) can be expressed as:

$$N(D|N_t, \mu, \Lambda) = \alpha N_t D^\mu e^{-\Lambda D}, \quad (1)$$

$$\text{with } \alpha = \left(\int_{D_{\min}}^{D_{\max}} D^\mu e^{-\Lambda D} dD \right)^{-1}$$

The number of drops $N(D)$ per unit volume and per diameter class depends on 3 parameters: the shape μ , the rate Λ and the total concentration N_t . These parameters are fitted using a Maximum Likelihood method. To quantify the spatial variability of the DSD during the event, the coefficient of variation (standard deviation divided by the mean, CV hereafter) of each parameter is calculated from the 16 measured values. For μ , Λ and N_t , mean CV values are about 25-30% indicating a significant variability within the 1x1 km² monitored area. The time series of CV for each parameter are presented in Figure 6 as well as the mean rain rate over the 16 stations. The highest CV values are observed during periods with rain intensity lower than 10 mm h⁻¹, i.e., mainly at the beginning and the end of the event. The maximum relative dispersion for μ , Λ and N_t are about 66, 83 and 112% respectively. These numbers indicate that there is a significant variability of the DSD within a radar pixel at 30 s time resolution. It must be noted that sampling errors can contribute to this variability when the observed DSD spectra correspond to a limited number of drops, i.e., light rain.

3.3 Variability of the $Z - R$ relationship

Conventional weather radar measure the reflectivity factor Z related to the electromagnetic properties of drops and convert it into rain rate R using the power law $Z = aR^b$. The prefactor a and the exponent b are often estimated using DSD measurements

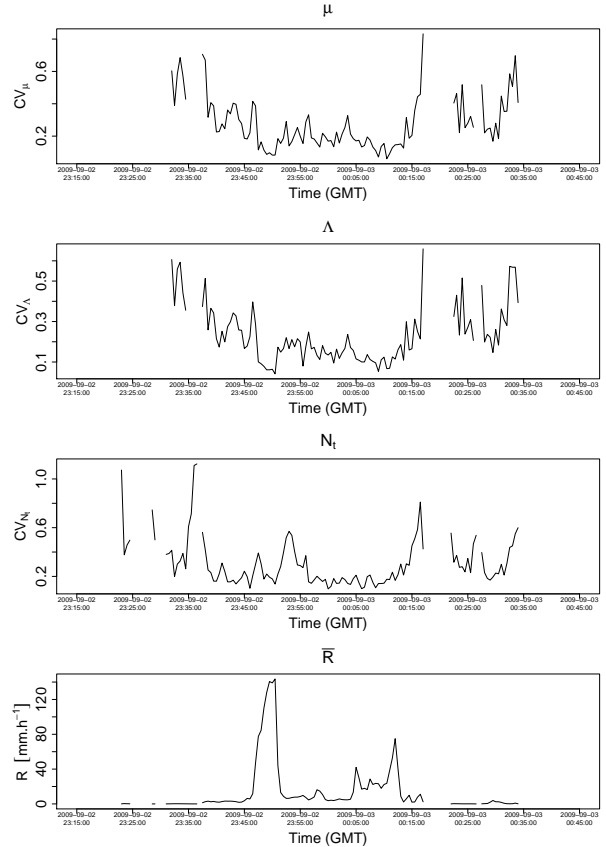


Figure 6: The coefficient of variation of the three parameters of the Gamma distribution: μ , Λ and N_t . The last graph is the rain rate averaged over the 16 stations. The gap in the signals are not considered due to the filtering process.

collected at the point scale. In order to investigate the variability of these parameters within a typical radar pixel, a and b are fitted on Z and R values at each station. The two parameters exhibit a significant variability between the stations with a range of a values from 225 (station 31) to 332 (station 33) and b values from 1.43 (station 13) to 1.49 (station 31). Figure 7 presents the couples (a,b) for each station as well as two characteristic points. The ensemble of all the point measurements (m) is calculated using the R and Z point values provided by all the stations. As expected, this ensemble point ($a=282$, $b=1.47$) is within the ranges of the single couples. A radar provides an estimation of the rain integrated over the scanned volume. Therefore, the a and b estimated using the pixel averaged (i.e., mean of 16 stations) \bar{R} and \bar{Z} values is more relevant for the conversion of the radar measured reflectivity into rain rate. For the considered event, $a=441$ and $b=1.37$.

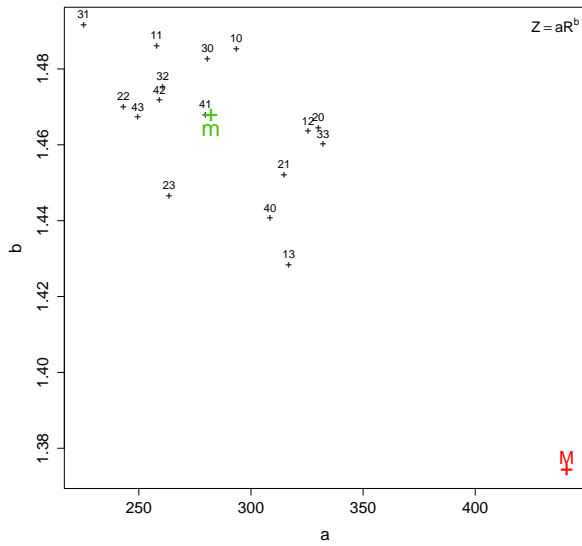


Figure 7: Variability of the a (X-axis) and b (Y-axis) parameters of the $Z - R$ relationship. The red M denotes the couple (a,b) estimated using the pixel averaged \bar{R} and \bar{Z} values while the green m point is calculated using all the R and Z point values given by the 16 stations.

The variability of a and b with respect to the average of point values (M point in Figure 7) are in the interval $[-49\%, -25\%]$ and $[+4\%, +8.5\%]$ respectively. This highlights the significant scale effect when comparing point measurements with measurements integrated over the pixel.

4 CONCLUSION

A wireless network of 16 optical disdrometers Parsivel has been designed and deployed over EPFL campus, Lausanne, Switzerland. This network is running for several months and different types of rain event have been collected. The preliminary analysis of a convective rain event that occurred in September 2009 is presented. The spatial variability of the DSD at the radar pixel scale is quantified as the coefficient of variation (between the 16 stations) of the 3 parameters of a Gamma distribution fitted on each observed DSD spectrum. On average, it is about 30%, indicating a significant variability at such a small scale ($1 \times 1 \text{ km}^2$). The $Z - R$ relationship used in data processing for non polarimetric radar exhibits as well a significant variability of its two parameters a and b . Such a variability in the $Z - R$ relationship with up/down scaling can yield significant biases in rain estimation

from radar. These preliminary investigations of the spatial variability of the DSD will be pursued. In particular, future work will investigate the influence of the sampling uncertainty associated with DSD measurement and fitting on the estimated natural DSD variability (of interest).

Acknowledgments. This research is supported by the Swiss National Science Foundation (grant 200021-118057/1).

REFERENCES

- Lee, C. K., G. Lee, I. Zawadzki, and K. Kim, 2009: A preliminary analysis of spatial variability of raindrop size distributions during stratiform rain events. *J. Appl. Meteor. Climate*, **48**, 270–283, doi:10.1175/2008JAMC1877.1.
- Lee, G. and I. Zawadzki, 2005: Variability of drop size distributions: time-scale dependence of the variability and its effects on rain estimation. *J. Appl. Meteor.*, **44**, 241–255, doi:10.1175/JAM2183.1.
- Löffler-Mang, M. and J. Joss, 2000: An optical disdrometer for measuring size and velocity of hydrometeors. *J. Atmos. Oceanic Technol.*, **17**, 130–139.
- Miriovsky, B., A. A. Bradley, W. E. Eichinger, W. F. Krajewski, A. Kruger, B. R. Neslon, J.-D. Creutin, J.-M. Lapetite, G. Lee, and I. Zawadzki, 2004: An experimental study of small-scale variability of radar reflectivity using disdrometer observations. *J. Appl. Meteor.*, **43**, 106–118.
- Tokay, A. and D. A. Short, 1996: Evidence from tropical raindrop spectra of the origin of rain from stratiform versus convective clouds. *J. Appl. Meteor.*, **35**, 355–371.
- Uijlenhoet, R., M. Steiner, and J. A. Smith, 2003: Variability of raindrop size distributions in a squall line and implications for radar rainfall estimation. *J. Hydrometeorol.*, **44**, 43–61.
- Ulbrich, C. W., 1983: Natural variations in the analytical form of the raindrop-size distribution. *J. Climate Appl. Meteor.*, **22**, 1764–1775.

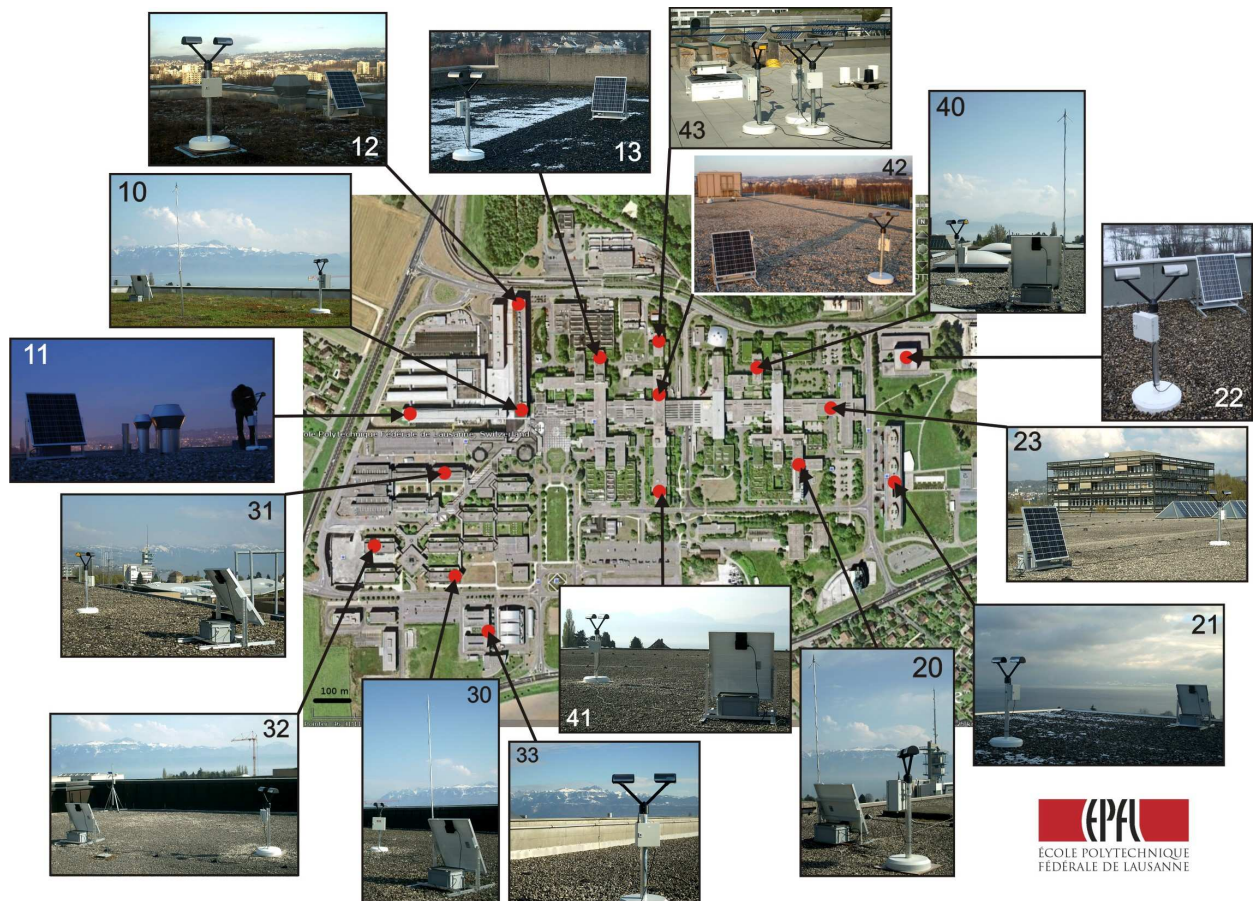


Figure 1: The network of 16 optical disdrometers deployed over EPFL campus ($\sim 1 \times 1 \text{ km}^2$) in Lausanne, Switzerland. The network is fully autonomous in terms of power supply and data transfer (wireless).

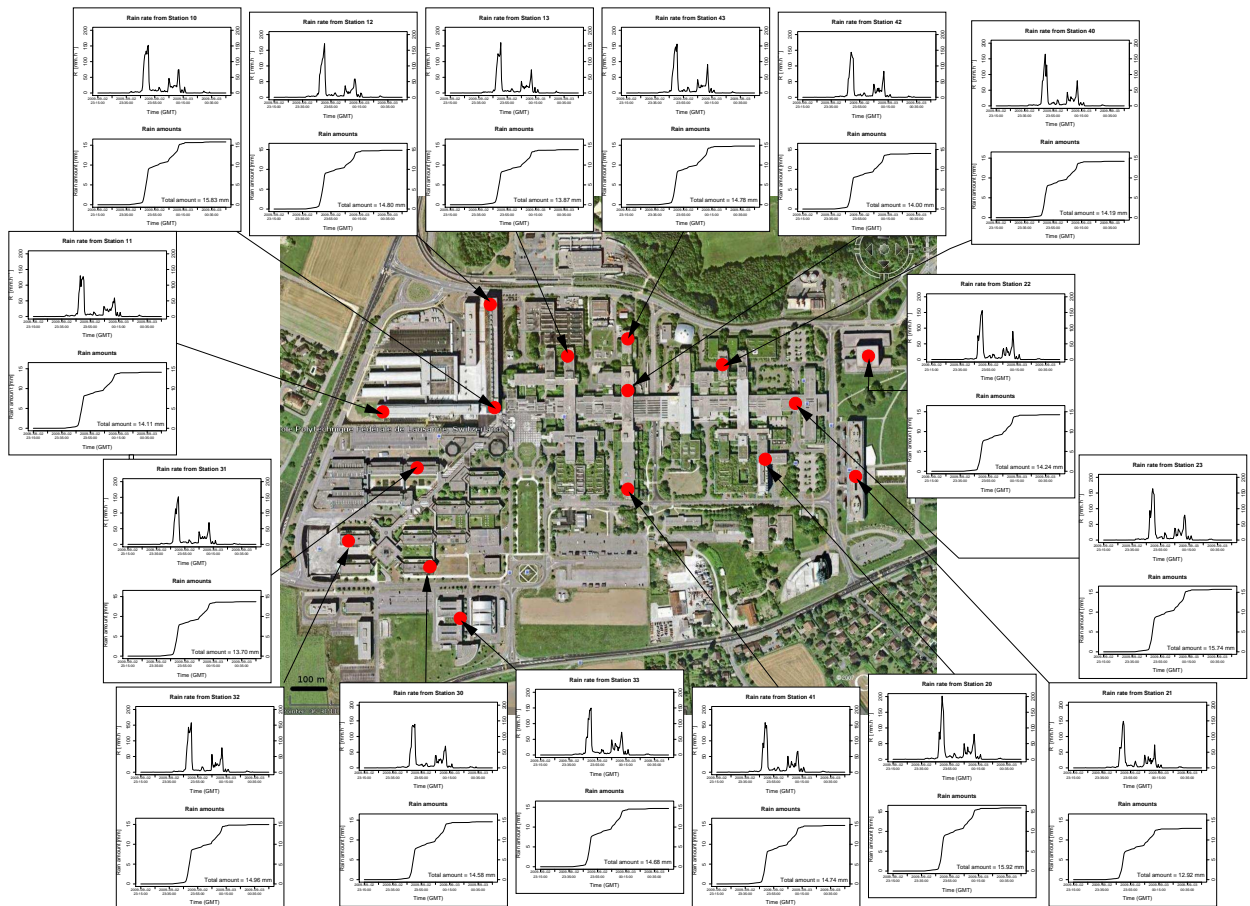


Figure 4: Rain rates (upper plots) and rain amounts (lower plots) recorded by each station during the rain event on the 3rd of September 2009 from 23:15 to 00:45 (GMT). The time resolution is 30 s.

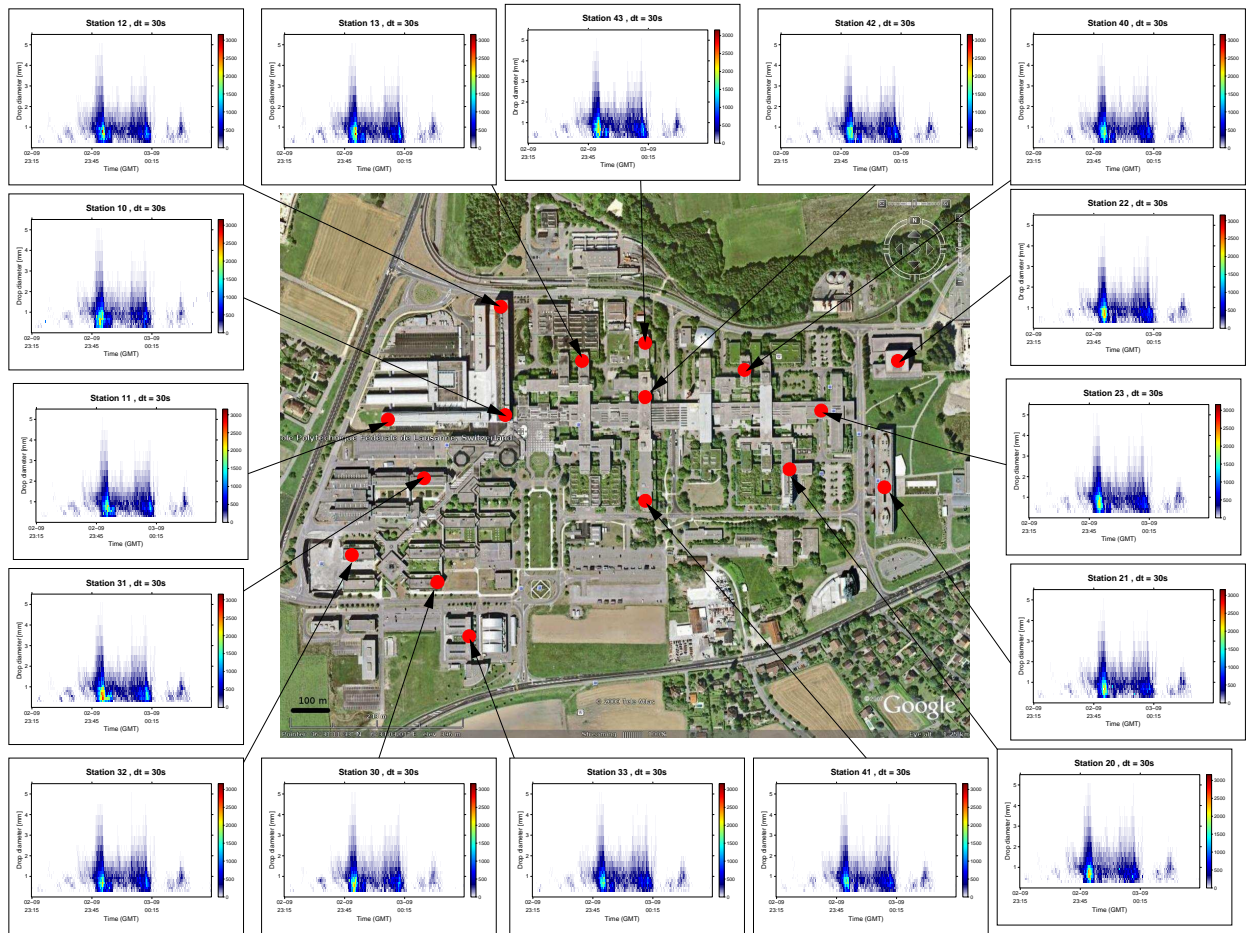


Figure 5: DSD spectra collected by each station during the rain event on the 3rd of September 2009 from 23:15 to 00:45 (GMT).